

Invisible Units Detection and Estimation Based on Random Matrix Theory

Xing He, Lei Chu, Robert C. Qiu, *Fellow, IEEE*, Qian Ai, Zenan Ling, Jian Zhang

Abstract—Invisible units mainly refer to small-scale units that are not monitored by, and thus are not visible to utilities. Integration of these invisible units into power systems does significantly affect the way in which a distribution grid is planned and operated. This paper, based on random matrix theory (RMT), proposes a statistical, data-driven framework to handle the massive grid data, in contrast to its deterministic, model-based counterpart. Combining the RMT-based data-mining framework with conventional techniques, some heuristics are derived as the solution to the invisible units detection and estimation task: linear eigenvalue statistic indicators (LEs) are suggested as the main ingredients of the solution; according to the statistical properties of LEs, the hypothesis testing is formulated to conduct change point detection in the high-dimensional space. The proposed method is promising for anomaly detection and pertinent to current distribution networks—it is capable of detecting invisible power usage and fraudulent behavior while even being able to locate the suspect’s location. Case studies, using both simulated data and actual data, validate the proposed method.

Index Terms—invisible unit, data-mining framework, statistical property, random matrix theory, linear eigenvalue statistic.

I. INTRODUCTION

FUTURE grids will be fundamentally different from current ones [1]. Technology development, environment pressure, and market reform have greatly spurred the deployment of distributed, renewable, and even plug-and-play units, on both the power generation and the power consumption sides. These units are mostly invisible to utilities—they are not monitored by, and thus are not visible to grid operators. 1) Accessing distributed units data into utility systems requires an enormous cost of data acquisition, communication, storage, calculation, and security [2]. 2) It is difficult to describe these units using a deterministic model; they are small in size but large in amount, and most of them are with high uncertainty or individuality. 3) Some behavior, such as power theft [3], unauthorized PV installation [4], and cyberattack [5], is essentially invisible.

Lack of visibility may cause incorrect planning and operation of power systems, and even worse, damage to system equipment and customer appliances. In an environment highly penetrated by invisible units, utilities face technical problems related to overvoltage, frequency control, back feeding flow, and other issues such as a rapid decrease in revenue. Moreover, the transparency of the grid is the basis for some advanced management such as dynamic scheduling, demand response.

To enhance the visibility of the network, distribution utilities have begun deploying data collectors such as phasor measurement units (PMUs) [6]. High resolution voltage and current measurements can be used in a plethora of applications for

monitoring, diagnostic, and control purposes, such as state estimation, customer profiling, and anomaly detection [7].

In the invisible units detection and estimation task, we deal with a large number (called N) of nodes simultaneously. Each node collects a massive data samples (called T) for a given period of observation. A classical statistic theory treats a fixed N only. This fixed N is called low-dimensional regime. In practice, we are interested in the case that N can vary arbitrarily in size compared with T . This fundamental requirement is the **primary driving force** for us to choose RMT as the analysis theory. Indeed, the **joint distribution** of the eigenvalues is analyzed by RMT as the statistic analytics from big data. To our best knowledge, RMT is developed to address this high-dimensional regime since the classical statistic theory applies to the low-dimensional regime only [8]. Our big data analytics exploit the high-dimensional phenomenon that occurs often in a modern grid. Our special view of angle is expected to contribute some novel algorithms to the community. The connection of our task with RMT may has deep impact on our community.

Lots of work has been done to study the impacts and risks of invisible units [9]. Little attention, however, has been paid to detection and estimation of said invisible units, especially in the context of a complex distributed grid. Some related works are found in the special issue of “Big Data Analytics for Grid Modernization” [10]. Reference [11] proposes a change-point detection algorithm, which is relevant to our paper to an extent. Reference [4] takes the uncertainty into account, and estimates the power generation of unauthorized PV installation using data generated from a small set of selected representative sites. Reference [12] proposes an approach for anomaly detection and causal impact analysis using a two-layer dynamic optimal synchrophasor measurement devices selection algorithm. Our previous work [1, 13, 14], based on RMT, outlines a data-driven framework of big data analytics for power systems. Our RMT-based framework, **via spectrum analysis**, studies the **statistical information which is unique in high-dimensional space**. Besides, the linear eigenvalue statistic (LES) and its statistical properties and advantages, as well as some RMT-relevant operations, are discussed.

A. Contribution

This paper aims at a challenging and pertinent task to current distribution networks—detection and estimation of invisible units. Combining the RMT-based data-mining framework with classical hypothesis testing techniques, some heuristics are derived as the solution to the task. RMT and the relevant

operations, which **perform well in uncertainty processing in high-dimensional space**, are employed to conduct feature extraction from the massive temporal-spatial data. Linear eigenvalue statistic indicators (LEs), which are **robust against data errors** (e.g., data loss, data out-of-synchronization [14]) and **insusceptible to random noises** (e.g., white noises [1]), are employed as the features. Based on the statistical properties of LEs, a hypothesis testing is formulated to conduct change point (CP) detection for invisible units modeling. The technical route for the task is given in Fig. 1 in Section III-G. The method is model-free and only relies on easily accessible utility data, yet it is effective and fairly powerful—Fig. 5 in Section IV-D shows that a much more accurate result is obtained using our method.

The remainder of this paper is organized as follows. Section II maps the invisible units detection and estimation task onto a mathematical model. Section III studies the mathematical tools to handle the aforementioned model, and then gives a full picture for the task. Section IV and V, with the simulated cases and real-system cases respectively, validate the proposed method. Section VI presents the conclusions of this research.

II. PROBLEM FORMULATION

A. Definition of TLPs and ULPs

This paper attempts to conduct invisible units detection and estimation in a non-omniscient distribution network. More precisely, we aim to obtain users (loads/generators) behavior and accordingly volume at the node level.

From the aspect of users behavior, the loads/generators are divided into two categories: typical load pattern units (TLPs) and uncertain load pattern units (ULPs).

- 1) TLPs operate according to well-defined profiles, which are denoted as vectors $\mathbf{p}_i^{(\alpha)}$. **TLPs' patterns are known in advance—they can be checked by the users based on the daily routine or learned via cluster algorithms using historic data** [15]. For instance, a street-lamp that is set turning on at 18:00 and turning off at 06:00 is a TLP; the street-lamp pattern is modeled as

$$\mathbf{p}^\xi(t) = \begin{cases} 1 & t \in [00 : 00, 06 : 00] \cup [18 : 00, 24 : 00] \\ 0 & t \in [06 : 00, 18 : 00] \end{cases}.$$

If the sampling interval is 6 hours, $\mathbf{p}^{(\xi)} = [1, 0, 0, 1]$.

- 2) ULPs are also expressed in time-series, which are denoted as vectors $\mathbf{p}_j^{(\beta)}$. Comparing to TLPs', **ULPs' patterns are not accessible in advance or predictable**. The aforementioned invisible units, such as plug-and-play EVs and climate-susceptible PVs, all belong to ULPs.

B. Classification of ULPs

ULPs can be further divided into three categories—random behavior, invisible behavior, and fraudulent behavior. Our previous work [1, 14], based on RMT, has already studied the random behavior, and verified that **the (independent) random behavior, e.g., white noises, has little impact on the value of LEs**. This paper focuses on the left two—the invisible

behavior and the fraudulent one. The examples of the both will be given and studied in Section IV-C.

The invisible behavior often causes a chain reaction and has an impact on numerous parameters. For instance, the PVs electricity generations do change the power flow of the grid network. The fraudulent behavior, however, often causes parameter deviation alone. For example, some metering errors or power thefts may merely distort the power consumption value P of some node without affecting other variables. **The differences between the two behavior above, from the aspect of mathematic, will be revealed by temporal-spatial correlations (among the multiple variables in time-series), which only exist in the high-dimensional space.**

C. Invisible Units Detection and Estimation Task Model

Considering the volume, we propose to study a general model for each node:

$$\underbrace{\mathbf{p}^{(\Sigma)}}_{\text{Observed Data}} = \underbrace{a_1 \mathbf{p}_1^{(\alpha)} + \cdots + a_n \mathbf{p}_n^{(\alpha)}}_{\text{Power Usage of TLPs}} + \underbrace{b_1 \mathbf{p}_1^{(\beta)} + \cdots + b_m \mathbf{p}_m^{(\beta)}}_{\text{Power Usage of ULPs}}, \quad (1)$$

where vectors $\mathbf{p}_i^{(\alpha)}$ stand for the daily patterns of TLPs, with the coefficients (volume) $a_i, i=1, \dots, n$, and accordingly, $\mathbf{p}_j^{(\beta)}$ for ULPs, with the coefficients $b_j, j=1, \dots, m$. As a result, vector $a_i \mathbf{p}_i^{(\alpha)}$ is the daily power usage for the i -th TLP, similarly vector $b_j \mathbf{p}_j^{(\beta)}$ for the j -th ULP.

For the invisible units detection and estimation task, the existence of ULPs need to be detected, and furthermore, the pattern of invisible units $\mathbf{p}_j^{(\beta)}$, as well as the coefficients (volume) a_i, b_j , need to be estimated.

If all units' pattern and behavior are known in advance, i.e., no $\mathbf{p}_j^{(\beta)}$ exists, or if ULPs are able to be modeled as routine $\mathbf{p}_{n+j}^{(\alpha)}$ instead of uncertain $\mathbf{p}_j^{(\beta)}$, then Eq. (1) is turned into

$$\mathbf{p}^{(\Sigma)} = a_1 \mathbf{p}_1^{(\alpha)} + a_2 \mathbf{p}_2^{(\alpha)} + \cdots + a_{n+m} \mathbf{p}_{n+m}^{(\alpha)}. \quad (2)$$

Eq. (2) can be solved through a systematic procedure.

$$\arg \min_{\mathbf{a}} \left\| \mathbf{P} \mathbf{a} - \mathbf{p}^{(\Sigma)} \right\| \quad (3)$$

where $\mathbf{P} = \begin{bmatrix} \mathbf{p}_1^{(\alpha)} & \cdots & \mathbf{p}_{n+m}^{(\alpha)} \end{bmatrix}$, $\mathbf{a} = [a_1 \ \cdots \ a_{n+m}]^T$.

Using the least squares method, the estimated value of \mathbf{a} is obtained as

$$\hat{\mathbf{a}} = (\mathbf{P}^T \mathbf{P})^{-1} \mathbf{P}^T \mathbf{p}^{(\Sigma)} \quad (4)$$

It is worth mentioning that the analysis of reactive power Q may be conducted in a similar way.

In a modern distribution network, ULPs $b_j \mathbf{p}_j^{(\beta)}$ are present and their influences need to be considered. The existence of ULPs violates the prerequisites of most algorithms (e.g., least squares method) and may cause significant bias on the estimated values of coefficients a_i starting from Eq. (4). **Without a fairly correct ULPs detection, spurious results may be obtained**, just as illustrated in Fig. 5 in Section IV-D.

In most scenarios, **it is reasonable to model $\mathbf{p}_j^{(\beta)}$ as a step signal**. This is the case when EVs charge or PVs generate during t_a to t_b . **Determining the start point t_a and the end point t_b of the step signal** is at the heart of $\mathbf{p}_j^{(\beta)}$ modeling.

III. MATHEMATICAL FOUNDATION

A. Random Matrix Theory

1) Statistics based on Random Matrix Theory:

Random matrices have been an important issue in multivariate statistical analysis since the landmark work of Wishart on fixed size Gaussian matrices. Asymptotic theory on the limiting spectrum of large random matrices was initially proposed in several works [16] by Wigner in the 1950s, motivated by problems in quantum physics. Since then, research on finite spectral analysis of high dimensional random matrices has come under heated discussion by scholars in numerous disciplines [8]. RMT, as a statistical tool with profound theoretical basis, is adapted to multivariate analysis. It can help model many intractable practical systems, especially those with numerous variables.

2) Laws for Spectral Analysis:

RMT says that for a Laguerre unitary ensemble (LUE) matrix $\mathbf{A} \in \mathbb{C}^{N \times T}$ ($c = N/T \leq 1$), its empirical spectral density (ESD) $g_{\mathbf{A}}(x)$ follows Marchenko-Pastur (M-P) Law [17]:

$$g_{\mathbf{A}}(x) = \frac{1}{2\pi cx} \sqrt{(x-a)(b-x)}, x \in [a, b] \quad (5)$$

where $a = (1 - \sqrt{c})^2$, $b = (1 + \sqrt{c})^2$.

3) Universality Principle of RMT:

This universality principle [18] enables us to obtain the exact asymptotic distributions of various test statistics **without restrictive distributional assumptions of matrix entries**. For a real system with massive temporal-spatial data, we cannot expect the matrix entries to follow i.i.d. distribution. **One can perform various hypothesis testings under the assumption that the matrix entries are not Gaussian distributed but use the same test statistics as in the Gaussian case**. Numerous studies using both grid network data [14] and power transmission equipment data [19] demonstrate that the M-P Law and Ring Law are universally valid—the asymptotic results are **remarkably accurate for engineering data with relatively moderate matrix sizes such as tens**. This is the very reason why RMT can handle practical massive systems.

B. Connection between RMT and our Task

1) Connection with Random Matrix Theory:

The observed data, given in Eq. (1), consist of multiple variables in time-series. And each variable, i.e., the data of a single node, is a mixture of multiple signals—noises (ULPs), given signals (TLPs), and unknown signals (ULPs). Under the view of the whole grid network, there should be some high-dimensional statistic information among these signals, **said temporal-spatial correlations**. Indeed, further division can be made; for instance, the noises can be divided into white noises and colored noises, and the given signals can be expressed in terms of diverse models such as those based on ARMA processes [19] and Ornstein-Uhlenbeck processes [20]. The division topic will be discussed elsewhere and this paper focuses on the step signal detection as mentioned in Section II-C, which is an essential anomaly detection task, by utilizing the temporal-spatial data via signal analysis algorithms designing.

The signal analysis algorithms are often designed based on the characteristics of the raw data. For instance, low rank matrix completion (LRMC) are based on low rank [21], and sparse principal component analysis (sparse PCA) based on sparsity [22]. Similarly, based on **the temporal-spatial correlations**, we propose our RMT-based framework.

The signal analysis aiming at extracting the informative statistics (big data analytics) from the massive data, as mentioned in Section I, **is a challenge that does not meet the prerequisites of most conventional tools**. The task has some connection with the field of communication, in particular, massive MIMO (Multiple-Input Multiple-Output) technology in work [23]. In the neighbor communication field, RMT has already been fully proved as an effective and popular tool through hundreds of thousands of published studies. In the field of power systems, however, there are much fewer RMT-relevant researches.

2) Connection with Other Potential Algorithms:

The supervised learning mode is also adapted to handle high-dimensional data. In a supervised learning context, ground truth data can be exploited to seek parameters automatically. For instance, the state-of-the-art deep learning algorithm does select some non-handcrafted features (called deep features) from the massive labeled dataset without much prior knowledge, so that it can be generalized to different cases without making significant modifications. The deep learning algorithm holds a competitive advantage over our paradigm. Our paradigm, however, has an advantage of **transparency**—the algorithm is deeply rooted in RMT. Unifying time and space through their ratio $c = T/N$, RMT deals with temporal-spatial data **mathematically rigorously**. Linear eigenvalue statistics (LESs), built from data matrices, **follow Gaussian distributions for very general conditions**, and other statistical variables are studied due to the **latest breakthroughs in probability** on the central limit theorems (CLTs) of those LESs. The statistical properties of these variables are mostly derivable and provable. In this sense, our work is fundamental in nature. Besides, **RMT performs well with moderate-size (unlabeled) data**, which is often true in engineering.

C. Linear Eigenvalue Statistics and its Central Limit Theorem

The LES τ of an arbitrary matrix $\mathbf{\Gamma} \in \mathbb{C}^{N \times N}$ is defined in [24, 25] via the continuous test function $\varphi: \mathbb{C} \rightarrow \mathbb{C}$,

$$\tau_{\varphi} = \sum_{i=1}^N \varphi(\lambda_i) = \text{Tr} \varphi(\mathbf{\Gamma}), \quad (6)$$

where the trace of the function of a random matrix is involved.

1) Law of Large Numbers:

The Law of Large Numbers tells us that $N^{-1}\tau_{\varphi}$ converges in probability to the limit

$$\lim_{N \rightarrow \infty} \frac{1}{N} \sum_{i=1}^N \varphi(\lambda_i) = \int \varphi(\lambda) \rho(\lambda) d\lambda, \quad (7)$$

where $\rho(\lambda)$ is the probability density function (PDF) of λ .

2) Central Limit Theorem:

CLT, as the natural second step, aims to study the fluctuations of LES.

Theorem III.1 (M. Sheherbina, 2009, [25]). *Consider a random matrix $\mathbf{X} \in \mathbb{R}^{N \times T}$ in $N \times T$ size, and \mathbf{M} is the covariance matrix $\mathbf{M} = \frac{1}{N} \mathbf{X} \mathbf{X}^H$. The CLT for \mathbf{M} is given as follows: Let the real valued test function φ satisfy condition $\|\varphi\|_{3/2+\varepsilon} < \infty$ ($\varepsilon > 0$). Then τ_φ as defined in Eq. (6), in the limit $N, T \rightarrow \infty, c = N/T \leq 1$, converges in the distribution to the Gaussian random variable with the mean $\mathbb{E}(\tau_\varphi)$, according to Eq. (7), and the variance:*

$$\sigma^2(\tau_\varphi) = \frac{2}{c\pi^2} \iint_{-\frac{\pi}{2} < \theta_1, \theta_2 < \frac{\pi}{2}} \psi^2(\theta_1, \theta_2) (1 - \sin \theta_1 \sin \theta_2) d\theta_1 d\theta_2 + \frac{\kappa_4}{\pi^2} \left(\int_{-\frac{\pi}{2}}^{\frac{\pi}{2}} \varphi(\zeta(\theta)) \sin \theta d\theta \right)^2, \quad (8)$$

where $\psi(\theta_1, \theta_2) = \frac{[\varphi(\zeta(\theta))]_{\theta=\theta_1}^{\theta=\theta_2}}{[\zeta(\theta)]_{\theta=\theta_1}^{\theta=\theta_2}}$, $[\zeta(\theta)]_{\theta=\theta_1}^{\theta=\theta_2} = \zeta(\theta_1) - \zeta(\theta_2)$, and $\zeta(\theta) = 1 + 1/c + 2/\sqrt{c} \sin \theta$; $\kappa_4 = \mathbb{E}(X_{ij}^4) - 3$ is the 4-th cumulant of entries of \mathbf{X} .

To study the convergence as a function of N , we study LES instead of the probability distribution of eigenvalues in Eq. (5). For an arbitrary test function with enough smoothness, LES τ (see it as a random variable Y) is a positive scalar random variable defined in Eq. (6). As $N \rightarrow \infty$, the asymptotic limit of its expectation, $\mathbb{E}(Y)$, is given in Eq. (7), and the asymptotic limit of its variance, $\sigma^2(Y)$, is given in Eq. (8). **These two equations are sufficient to study the scalar random variable Y . This approach can be viewed as a dimensionality reduction**—the random data matrix of size $N \times T$ is reduced to a positive scalar random variable Y ! This dimension reduction is mathematically rigorous only when $N, T \rightarrow \infty$ but $\frac{N}{T} \rightarrow c$. **Experiences demonstrate, however, that moderate values of N and T are accurate enough for our practical purposes.**

D. LES-based Hypothesis Testing Designing for CP Detection

Change-point (CP) detection began with Page's (1954, 1955) classical formulation, which was further developed by Shiryaev (1963) and Lorden (1971) [26]. CP detection is the following problem: suppose X_1, X_2, \dots, X_m are independent observations. For $j \leq M$, they have distribution F_0 ; for $j > M$, they have distribution F_1 . The distributions F_1 may be completely specified or may depend on unknown parameters. In the case of a fixed number m of observations, we would like to test the null hypothesis of no change, that $F_0 = F_1$, and to estimate M .

This paper formulates the hypothesis testing, for the massive dataset, in terms of the statistical properties of LES. As aforementioned, LES, in the limit $N, T \rightarrow \infty, c = N/T \leq 1$, converges in the distribution to a Gaussian random variable τ_φ with mean $\mathbb{E}(\tau_\varphi)$, according to Eq. (7), and variance $\sigma^2(\tau_\varphi)$, according to Eq. (8). Moreover, our previous work shows that LES is **robust against data errors** (e.g., data loss, data out-of-synchronization [14]) and **insusceptible to (independent) random noises** (not limited to white noises [1]), which is **not true to those low dimensional statistics** such as mean and variance of any single variable. All of these statistical

properties **make LES a good feature** for a hypothesis testing designing aiming at anomaly detection task.

Referring the Gaussian property and standard scores [27]¹, the detection is modeled as a binary hypothesis testing: the normal hypothesis \mathcal{H}_0 (no anomaly present) and the abnormal one \mathcal{H}_1 , denoted by:

$$\begin{cases} \mathcal{H}_0 : \left| \frac{\tau_\varphi - \mathbb{E}(\tau_\varphi)}{\sigma(\tau_\varphi)} \right| < \epsilon, \\ \mathcal{H}_1 : \left| \frac{\tau_\varphi - \mathbb{E}(\tau_\varphi)}{\sigma(\tau_\varphi)} \right| \geq \epsilon, \end{cases} \quad (9)$$

where ϵ is a threshold value that needs to be preset.

It is worth mentioning that the aforementioned Gaussian property and standard scores do offer a reference for setting the threshold value ϵ ; for instance, at a significance level 0.05, the ϵ should be set at 1.96. However, when setting the threshold range for possible applications in the real world, we should take account of many other factors, e.g., the performance of the real-time $\tau_\varphi - t$ curve, the experiment with the historical data, the experience of the problem solver, and other statistical hypothesis testings such as Student's t -test.

E. Matrices Concatenation Operation

Numerous **causing factors** affect the **system state** in different ways. Sensitivity analysis is a valuable and hot topic. The sampling data are in the form of multiple time-series, and we assume that there are N state variables and M factors. Within a fixed period of interest t_i ($i = 1, \dots, T$), the sampling data of N state variables consist of matrix $\mathbf{B} \in \mathbb{C}^{N \times T}$ (i.e. **state matrix**), and the factors consist of vector $\mathbf{c}_j^T \in \mathbb{C}^{1 \times T}$ ($j = 1, \dots, M$) (i.e. **factor vector**). Two matrices with the same length can be put together and thus a new concatenated matrix is formed. In such a way, matrix \mathbf{A}_j is formed by concatenating state matrix \mathbf{B} with factor vector \mathbf{c}_j^T .

In order to balance the proportion (to increase statistic correlation), a factor matrix \mathbf{C}_j is formed by duplicating each factor vector \mathbf{c}_j^T for K times², written as

$$\mathbf{C}_j = [\mathbf{c}_j \quad \mathbf{c}_j \quad \dots \quad \mathbf{c}_j]^T \in \mathbb{C}^{K \times T}.$$

Then, white noise is introduced into \mathbf{C}_j to avoid extremely strong cross-correlations. Thus, factor matrix \mathbf{D}_j for factor vector \mathbf{c}_j^T is expressed as

$$\mathbf{D}_j = \mathbf{C}_j + \eta_j \mathbf{R} \quad (j = 1, 2, \dots, m), \quad (10)$$

where η_j is related to signal-to-noise ratio (SNR), and matrix \mathbf{R} is a standard Gaussian Random Matrix.

In parallel, we construct concatenated matrix \mathbf{A}_j with each factor \mathbf{c}_j^T , expressed as

$$\mathbf{A}_j = \begin{bmatrix} \mathbf{B} \\ \mathbf{D}_j \end{bmatrix} \in \mathbb{C}^{(N+K) \times T} \quad (j = 1, 2, \dots, m). \quad (11)$$

¹Standard scores are also called z-values, z-scores, normal scores, and standardized variables. They are most frequently used to compare an observation to a theoretical deviate, such as a standard normal deviate.

²Empirically, $K \approx 0.3 \times N$. [13]

Relationships between causing factors \mathbf{c}_j^T and system state \mathbf{B} can be revealed by concatenated matrix \mathbf{A}_j . This concatenated model is compatible with different units and different measurements for each variable data which are in the form of rows of \mathbf{A}_j , due to the normalization during data preprocessing. It is worth mentioning that some mathematical methods, e.g., interpolation, may be applied to handle sensor data with different sampling rates.

F. Experiment Design for Power Systems

For power systems, voltage magnitudes U and power consumptions P are preferred for the following reasons: 1) they are easily accessible and usually at a high accuracy; 2) they belong to measurement parameters, which are independent from network topology; and 3) our previous work [1] proves that, for certain scenarios, different types of streaming data, such as V and I , may have similar statistical properties in high dimensional space. Similar to Eq. (11), \mathbf{F}_j is formed as

$$\mathbf{F}_j = \begin{bmatrix} \mathbf{U} \\ \mathbf{P}_j^{(\Sigma)} \end{bmatrix} \in \mathbb{C}^{(N+K) \times T} \quad (j = 1, 2, \dots, N). \quad (12)$$

The state matrix $\mathbf{U} \in \mathbb{C}^{N \times T}$ consists of voltage magnitudes $[U]_{j,t} (j = 1, \dots, N, t = 1, \dots, T)$, and the j -th factor matrix $\mathbf{P}_j^{(\Sigma)} \in \mathbb{C}^{K \times T}$ consists of active power consumptions $[P_j^{(\Sigma)}]_{k,t} (j = 1, \dots, N, k = 1, \dots, K, t = 1, \dots, T)$ according to Eq. (10).

G. Technical route for Detection and Estimation Task

Concluding Section II and III, we outline the flowchart to make a full picture of processes for the invisible units detection and estimation task, as shown in Fig. 1.

With the technical route given in Fig. 1, we make a progress to our task from the conventional techniques such as change point detection and least squares methods. **Employing RMT-based framework, our method conducts big data analytics mathematically rigorously to the massive dataset.** Based on spectrum analysis, some statistical properties **which are unique in high-dimensional space** are utilized. For instance, to the statistic LES, its value is robust against data errors and insusceptible to random noises as said in Section III-D, but it is not true to those low dimensional statistics such as mean and variance of any single variable. That is a major reason why we choose RMT-based framework and LESs.

Fig. 5 validates the effectiveness of the proposed method—**a much more accurate estimation of coefficient values for the components is obtained.**

IV. SIMULATION CASES

A. Background

Simulations are based on an IEEE-33 System for a distribution network. For Node $j (j = 1, \dots, 33)$, its gross power usage $\mathbf{p}_j^{(\Sigma)}$ and voltage magnitude \mathbf{u}_j are sampled at a high rate, for example, 9600 points per day (0.11 Hz). The white noise is added to the power injections as

$$\tilde{y}_{nt} = y_{nt} (1 + \gamma_1 z_1) + \gamma_2 z_2, \quad (13)$$

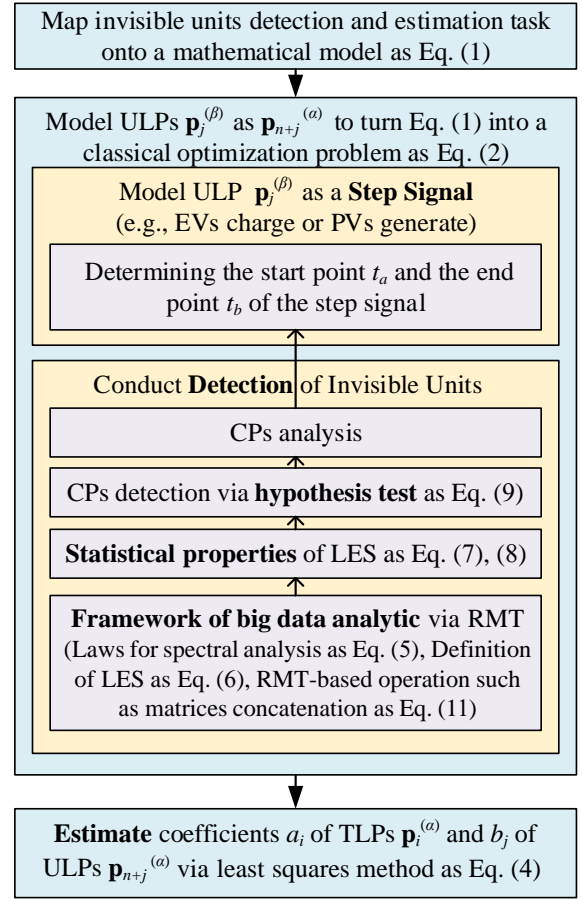


Fig. 1: Flowchart of RMT-based detection and estimation task

where z_1 and z_2 are two standard Gaussian random variables, i.e. $z_1, z_2 \sim \mathcal{N}(0, 1)$; $\gamma_1 = 0.005$, $\gamma_2 = 0.02$. In this way, the power flow is obtained via Matpower [28].

As mentioned in Sec. II, we mainly focus on fraudulent behavior and invisible power usage. Determining the start point and the end point of $\mathbf{p}_i^{(\beta)}$ is the main focus of this study. For longstanding anomalies without sudden change in the observed data segment, some long-term indicators, such as monthly line loss rate, might be effective.

B. Fraud events in a Simple Scenario

Fraud events often cause parameter deviation alone. Suppose that active power values P for each node stay around their initial points with fluctuations given as Eq. (13). From 14:00 to 17:00, some fraud events on Node 6 and Node 14 cause a reduction of 0.005 MW (8.33% of P_6 , 4.17% of P_{14}), as shown in Fig. 2. The lines with legends *data 1* to *data 33* are for the actual power consumption on Node 1 to Node 33, and the lines with legends *data 34* and *data 35* are for the measured power consumption on Node 14 and Node 6, respectively. Note that due to the fraud events, the data with legends *data 14* and *data 6* are not accessible.

Matrices concatenation operation and moving split window analysis are employed for data analysis. According to Eq. (6), we make $N = 33$, $T = 100$, $\Delta T = 1$, and choose Chebyshev

polynomials $T_2: \varphi(x) = 2x^2 - 1$ as the test function. LESs of state matrix \mathbf{B} and concatenated matrix \mathbf{A}_j ($j = 1, \dots, 33$, referring to Eq. (12)) are obtained in Fig. 3.

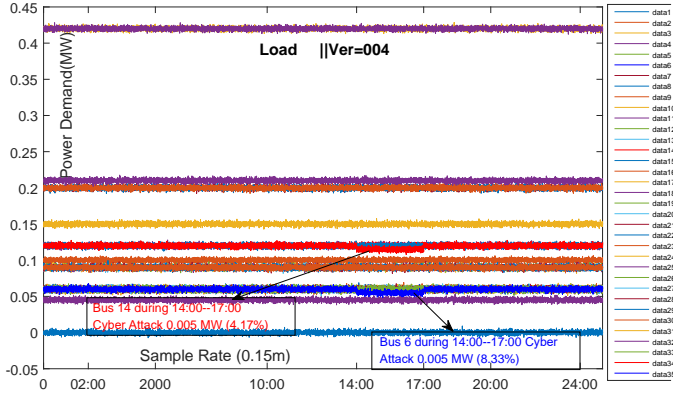


Fig. 2: Power demand P of each node

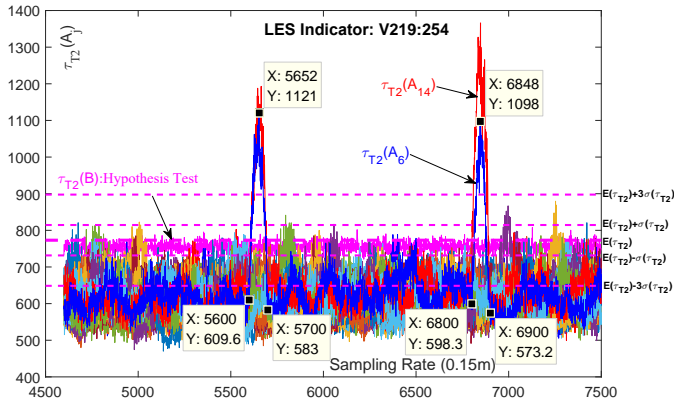


Fig. 3: LESs in the simple scenario

In Fig. 3, LES τ_{T_2} of state matrix \mathbf{B} , namely, $\tau_{T_2}(\mathbf{B})$ is almost constant. From a statistical view, the theoretical expectation $\mathbb{E}(\tau_{T_2})$ and the standard deviation $\sigma(\tau_{T_2})$ are accessible via random matrix theory, or rather, via Eq. (7) and (8). It is found that the experimental indicator $\tau_{T_2}(\mathbf{B})$ is exactly bounded between $\mathbb{E}(\tau_{T_2}) - 1.96\sigma(\tau_{T_2})$ and $\mathbb{E}(\tau_{T_2}) + 1.96\sigma(\tau_{T_2})$. According to Eq. (9), we cannot reject the null (\mathcal{H}_0)—there is no factor actually affecting the system state during the observation period. On the other hand, the τ_{T_2} of state matrix \mathbf{A}_i , namely, $\tau_{T_2}(\mathbf{A}_i)$ has four spikes: two spikes for $\tau_{T_2}(\mathbf{A}_6)$ and two spikes for $\tau_{T_2}(\mathbf{A}_{14})$. Our previous work [1] tells us that the anomaly signal should last for T time points (i.e. $T \times 0.15$ minutes) and have an extreme point at $T/2$. This phenomenon is observed on the $\tau_{T_2}(\mathbf{A}_6) - t$ curve and $\tau_{T_2}(\mathbf{A}_{14}) - t$ curve: $5700 - 5600 = 100 = T$, $5652 - 5600 \approx 50 = T/2$.

C. Invisible Unit Detection in a Complex Scenario

This subsection, focusing on fraudulent behavior and invisible behavior, proposes a data-driven solution to the task given in Sec. II—determining the start point and the end point to model the invisible unit $\mathbf{p}_j^{(\beta)}$ as a step signal. Firstly, the following assumptions are made:

- (I) Power usage on Node j ($j = 1, \dots, 33$) generally consists of four TLPs and one ULP, denoted as

$$\mathbf{p}_j^{(\Sigma)} = a_{j1}\mathbf{p}_1^{(\alpha)} + \dots + a_{j4}\mathbf{p}_4^{(\alpha)} + b_{j1}\mathbf{p}_1^{(\beta)}. \quad (14)$$

Daily load profiles of TLPs ($\mathbf{p}_1^{(\alpha)}, \dots, \mathbf{p}_4^{(\alpha)}$) are set as Tab. I and shown in Fig. ???. Note that the blue-filled rectangle indicates that the load profile has a dramatic change at this time point, i.e., change point (CP) [11].

- (II) Coefficients a_i, b_j ($i = 1, 2, 3, 4; j = 1$) are set as Tab II.
 (III) Invisible power usage events exist on Node 20 and 31: the periods are 1:00–5:00 and 14:00–20:00, and the percentages are 30% and 50%, respectively.
 (IV) Fraud events exist on Node 6, 14 and 27: the periods are 20:00–22:00, 14:00–17:00 and 18:00–19:00, and the percentages are 7%, 8% and 12%, respectively.

	P1	P2	P3	P4	Pu1		P1	P2	P3	P4	Pu1
0	88	20	25	100	0	12	94	77	35	0	0
1	87	20	23	100	100	13	86	80	30	0	0
2	88	20	22	100	100	14	86	86	33	0	100
3	100	21	22	100	100	15	88	86	44	0	100
4	96	20	27	100	100	16	85	87	50	100	100
5	100	20	31	100	0	17	87	35	56	100	100
6	98	20	29	0	0	18	88	25	85	100	100
7	97	30	28	0	0	19	85	25	80	100	100
8	88	40	31	0	0	20	84	20	70	100	0
9	82	85	37	0	0	21	83	20	76	100	0
10	82	85	42	0	0	22	86	20	43	100	0
11	95	82	42	0	0	23	88	15	30	100	0

Note: blue-filled rectangle indicates CP.

TABLE I: TLPs, ULPs and their 24-hour power demands.

TABLE II: Coefficients of TLPs and ULP of each node.

	a1	a2	a3	a4	b1		a1	a2	a3	a4	b1
1	0.25	0.25	0.25	0.25	0	2	0	0.7	0.1	0.2	0
3	0	0.1	0.8	0.1	0	4	0.05	0.75	0.1	0.1	0
5	0	0.1	0.8	0.1	0	6	0.1	0.2	0.5	0.2	0
7	0.8	0.05	0.1	0.05	0	8	0.85	0.05	0	0.1	0
9	0.1	0.15	0.6	0.15	0	10	0	0.15	0.8	0.05	0
11	0	0.2	0.75	0.05	0	12	0.05	0.1	0.75	0.1	0
13	0.05	0.05	0.85	0.05	0	14	0.7	0.05	0.2	0.05	0
15	0	0.05	0.9	0.05	0	16	0	0	0.95	0.05	0
17	0	0.1	0.8	0.1	0	18	0	0.7	0.1	0.2	0
19	0	0.5	0.1	0.4	0	20	0	0.2	0.2	0.3	0.3
21	0	0.8	0.1	0.1	0	22	0.1	0.75	0	0.15	0
23	0.2	0.6	0	0.2	0	24	0.85	0	0.05	0.1	0
25	0.75	0.1	0.1	0.05	0	26	0.2	0	0.7	0.1	0
27	0.1	0	0.75	0.15	0	28	0.25	0.1	0.6	0.05	0
29	0.8	0.05	0.1	0.05	0	30	0.9	0	0.05	0.05	0
31	0.1	0.1	0.05	0.25	0.5	32	0.9	0	0	0.1	0
33	0.95	0	0	0.05	0						

In the assumed complex scenario above, the active power P and the voltage U of each node are accessible, as shown in Fig. 4a and 4b, respectively. Following Eq. (12), \mathbf{F}_j is obtained for Node j ($j = 1, \dots, 36$). The LESs of \mathbf{F}_j are obtained as the $\tau_{T_2} - t$ curves shown in Fig. 4c and Fig. 4d.

These figures give a visualization of LESs throughout a whole day. Particular attention should be paid to the spikes—their corresponding time point and line number hold vital clues about when and where the behavior occurs:

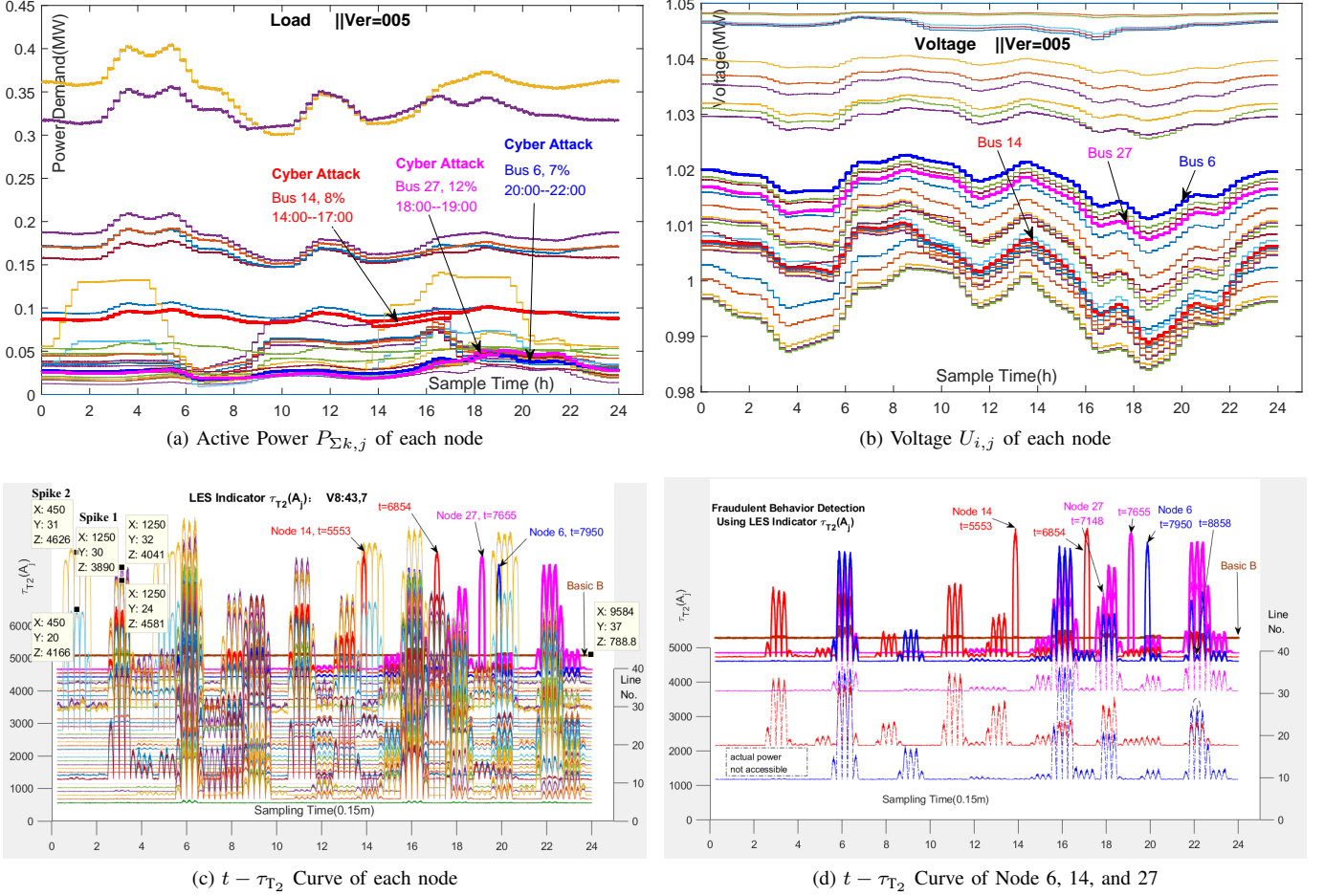


Fig. 4: Illusion of the data and analysis of a complex scenario for behavior analysis.

- The brown line indicates $\tau_{T_2}(\mathbf{B})$; it is relatively smooth because the system is stable without emergencies such as voltage collapse. Our previous work [1] verifies that the independent random noises ,e.g., completely random behavior, has little impact on the value of LESs.
- For fraud events, the extreme points are located at $t = 5553, 6854, 7655$, etc. According to Section IV-B, this phenomenon **matches Assumption IV** that the CPs are at $t = 14:00(5600 \approx 5553+50)$, $17:00(6800 \approx 6854-50)$, $19:00(7600 \approx 7655-50)$, etc., respectively.
- For TLPs, *Spike 1* ($X: 1250, Y: 32, Z: 4041$) indicates the existence of a CP at 3 : 00($1200 = 1250-50$) on Node 32. According to Tab. I, 3:00 is a CP of TLP $\mathbf{p}_1^{(\alpha)}$. Thus we can deduce that TLP $\mathbf{p}_1^{(\alpha)}$ takes a dominant on Node 32. Similar deductions can be made for Node 25, 24, 30, etc. These deductions **match Assumption are confirmed by Tab. II**.
- For invisible ULPs, *Spike 2* ($X: 450, Y: 31, Z: 4626$) indicates the existence of a CP at 1 : 00($400 = 450-50$) on Node 31. According to Tab. I, there is no existence of any TLP ($\mathbf{p}_1^{(\alpha)}, \mathbf{p}_2^{(\alpha)}, \mathbf{p}_3^{(\alpha)}, \mathbf{p}_4^{(\alpha)}$) matching CP 1:00. As a result, we artificially build a CP at 1:00 for a new ULP ($\mathbf{p}_1^{(\beta)}$ for this case). Step by step, all the CPs

of ULP $\mathbf{p}_1^{(\beta)}$ are obtained as Tab. I. Then, the general model Eq. (14) is tuned into the classical model Eq. (2) $\mathbf{p}^{(\Sigma)} = a_1\mathbf{p}_1^{(\alpha)} + a_2\mathbf{p}_2^{(\alpha)} + a_3\mathbf{p}_3^{(\alpha)} + a_4\mathbf{p}_4^{(\alpha)} + a_5\mathbf{p}_5^{(\alpha)}$.

D. Estimation with and without Invisible Units Detection

Existence of invisible units disables the classical least squares method. Taking Node 20 for instance, without correct detection of the invisible units, we will get a bad result as shown in Fig. 5. However, if the information about the start point and end point of the invisible behavior is acquired, an accurate estimate can be obtained.

V. REAL-WORLD CASE STUDIES

1) *Data*: A power grid with 5 substations in China is studied in this section as shown in Fig. 6a. For each substation, its three-phase voltage data V and current data I are recorded at a three-minute sampling-rate. We take a two-day time period as the dataset, depicted in Fig. 6c, 6d, 6e, and 6f.

2) *Ring Law and LES*: If we choose \mathbf{X}_0 (the voltage data during 0 a.m. to 2 a.m, Fig. 6c), the ring distribution is obtained according to our previous work [1], as shown in Fig. 6b. Most eigenvalues are distributed between the inner circle and the outer circle. This implies that the real-world data do

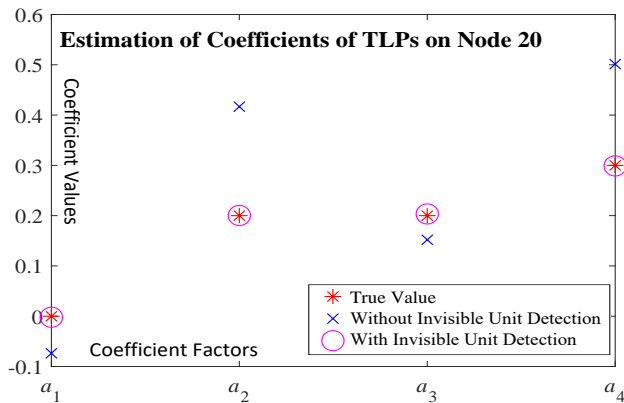


Fig. 5: Estimate with and without Invisible Units Detection

follow the Ring Law. With a similar process, and setting the test function as Chebyshev Polynomials T_2 : $\varphi_{T_2}(x) = 2x^2 - 1$ and the Likelihood Ratio Function LR: $\varphi_{LR}(x) = x - \ln(x) - 1$, respectively³, the LES $t-\tau$ curves are obtain in Fig. 7a, 7b, 7c, and 7d. The grid is relatively smooth during 0 a.m. to 8 a.m. and has dramatic changes at around 8:30 a.m., 11:30 a.m., etc. This observation agrees with our common sense. For field data, the test function may influence the results in some complicated ways, although the LESs have a similar trend at most CPs.

VI. CONCLUSION

This paper extends our framework of using large random matrices to model a power grid. Under the RMT-based framework, a progress, aiming at the invisible units detection and estimation task, is made from the conventional techniques such as change point detection and least squares methods, and detailed algorithms are given. Linear Eigenvalue Statistic (LES), whose value is robust against data errors and unsusceptible to random noises, is employed as the statistic feature (or big data analytics). Due to the high-dimensional phenomenon—arising from considering a large number of nodes simultaneously, LES is very appealing due to its Gaussian property implying that the expectation $\mathbb{E}(\tau)$ and the variance $\sigma^2(\tau)$ are sufficient for a complete statistic description. As a result, LES maps the massive datasets into a standard Gaussian random variable that is standard in classical statistics. The fundamental role of LES is highlighted here. As an example of how LES is used, we consider a standard (binary) hypothesis testing for invisible unit modeling. In particular, both the fraudulent behavior, e.g., false data injection, and anomalous power usage, e.g., unauthorized PV installation, are studied.

Based on mathematically rigorous RMT, time and space must be **tyed together** through their ratio $c = T/N$. What matters is the ratio c , rather than N and T . This observation is valid when N and T are large (for some statistical properties, size of tens is enough) and comparable in size, which is often true in practice.

³Our previous work [14] discusses the effectiveness of the choice of test functions. $\varphi_{T_2}(x)$ performs well on the calculation speed, and $\varphi_{LR}(x)$ performs well on the coefficient of variation in some cases.

Simulated data and real-world data are tested using our algorithms. It is found that the experimental values of LESs agree with the theoretical predictions. The proposed method does provide a data-driven approach to gain insight into the distribution network behavior and consumer profile, and a much more accurate estimation result is obtained.

REFERENCES

- [1] X. He, Q. Ai, R. C. Qiu, W. Huang, L. Piao, and H. Liu, "A big data architecture design for smart grids based on random matrix theory," *IEEE Transactions on Smart Grid*, vol. 8, no. 2, pp. 674–686, 2017.
- [2] J. Hu and A. V. Vasilakos, "Energy big data analytics and security: Challenges and opportunities," *IEEE Transactions on Smart Grid*, vol. 7, no. 5, pp. 2423–2436, 2016.
- [3] V. Gaur and E. Gupta, "The determinants of electricity theft: An empirical analysis of indian states," *Energy Policy*, vol. 93, pp. 127–136, 2016.
- [4] H. Shaker, H. Zareipour, and D. Wood, "Estimating power generation of invisible solar sites using publicly available data," *IEEE Transactions on Smart Grid*, vol. 7, no. 5, pp. 2456–2465, Sept 2016.
- [5] R. Deng, G. Xiao, R. Lu, and H. Liang, "False data injection on state estimation in power systems—attacks, impacts, and defense: A survey," *IEEE Transactions on Industrial Informatics*, vol. 13, no. 2, pp. 411–423, 2017.
- [6] A. Von Meier, D. Culler, A. McEachern, and R. Arghandeh, "Micro-synchrophasors for distribution systems," in *Innovative Smart Grid Technologies Conference (ISGT), 2014 IEEE PES*. IEEE, 2014, pp. 1–5.
- [7] O. Ardakanian, Y. Yuan, R. Dobbe, A. von Meier, S. Low, and C. Tomlin, "Event detection and localization in distribution grids with phasor measurement units," *arXiv preprint arXiv:1611.04653*, 2016.
- [8] R. Qiu and P. Antonik, *Smart Grid and Big Data*. John Wiley and Sons, 2015.
- [9] A. Samadi, L. Söder, E. Shayesteh, and R. Eriksson, "Static equivalent of distribution grids with high penetration of pv systems," *IEEE Transactions on Smart Grid*, vol. 6, no. 4, pp. 1763–1774, 2015.
- [10] T. Hong, C. Chen, J. Huang, N. Lu, L. Xie, and H. Zareipour, "Guest editorial big data analytics for grid modernization," *IEEE Transactions on Smart Grid*, vol. 7, no. 5, pp. 2395–2396, Sept 2016.
- [11] X. Zhang and S. Grijalva, "A data-driven approach for detection and estimation of residential pv installations," *IEEE Transactions on Smart Grid*, vol. 7, no. 5, pp. 2477–2485, Sept 2016.
- [12] H. Jiang, X. Dai, D. W. Gao, and J. J. Zhang, "Spatial-temporal synchrophasor data characterization and analytics in smart grid fault detection, identification, and impact causal analysis," *IEEE Transactions on Smart Grid*, vol. 7, no. 5, pp. 2525–2536, Sept 2016.
- [13] X. Xu, X. He, Q. Ai, and C. Qiu, "A correlation analysis method for power systems based on random matrix theory," *IEEE Transactions on Smart Grid*, vol. 8, no. 4, pp. 1811–1820, 2017.

- [14] X. He, R. C. Qiu, Q. Ai, L. Chu, X. Xu, and Z. Ling, "Designing for situation awareness of future power grids: An indicator system based on linear eigenvalue statistics of large random matrices," *IEEE Access*, vol. 4, pp. 3557–3568, 2016.
- [15] G. Chicco, "Overview and performance assessment of the clustering methods for electrical load pattern grouping," *Energy*, vol. 42, no. 1, pp. 68–80, 2012.
- [16] E. P. Wigner, "On the distribution of the roots of certain symmetric matrices," *Annals of Mathematics*, vol. 67, no. 2, pp. 325–327, Mar. 1958.
- [17] V. A. Marčenko and L. A. Pastur, "Distribution of eigenvalues for some sets of random matrices," *Sbornik: Mathematics*, vol. 1, no. 4, pp. 457–483, 1967.
- [18] R. van Handel, "Probability in high dimension," Princeton University, ORF 570 Lecture Notes, June 2014.
- [19] Y. Yan, G. Sheng, R. C. Qiu, and X. Jiang, "Big data modeling and analysis for power transmission equipment: A novel random matrix theoretical approach," *IEEE Access*, vol. 6, pp. 7148–7156, 2018.
- [20] M. Perninge, M. Amelin, and V. Knazkins, "Load modeling using the ornstein-uhlenbeck process," in *2008 IEEE 2nd International Power and Energy Conference*. IEEE, 2008, pp. 819–821.
- [21] P. Jain, P. Netrapalli, and S. Sanghavi, "Low-rank matrix completion using alternating minimization," in *Proceedings of the forty-fifth annual ACM symposium on Theory of computing*. ACM, 2013, pp. 665–674.
- [22] H. Zou, T. Hastie, and R. Tibshirani, "Sparse principal component analysis," *Journal of computational and graphical statistics*, vol. 15, no. 2, pp. 265–286, 2006.
- [23] C. Zhang and R. C. Qiu, "Massive mimo as a big data system: Random matrix models and testbed," *IEEE Access*, vol. 3, pp. 837–851, 2015.
- [24] A. Lytova, L. Pastur *et al.*, "Central limit theorem for linear eigenvalue statistics of random matrices with independent entries," *The Annals of Probability*, vol. 37, no. 5, pp. 1778–1840, 2009.
- [25] M. Shcherbina, "Central limit theorem for linear eigenvalue statistics of the wigner and sample covariance random matrices," *ArXiv e-prints*, Jan. 2011. [Online]. Available: <http://arxiv.org/pdf/1101.3249.pdf>
- [26] D. Siegmund, "Change-points: From sequential detection to biology and back," *Sequential Analysis*, vol. 32, no. 1, pp. 2–14, 2013.
- [27] Wikipedia, "Standard score," 2019. [Online]. Available: https://en.wikipedia.org/wiki/Standard_score
- [28] R. Zimmerman, C. Murillo-Sánchez, and D. Gan, "Matpower User's Manual, Version 4.1," *Power Systems Engineering Research Center*, 2011.

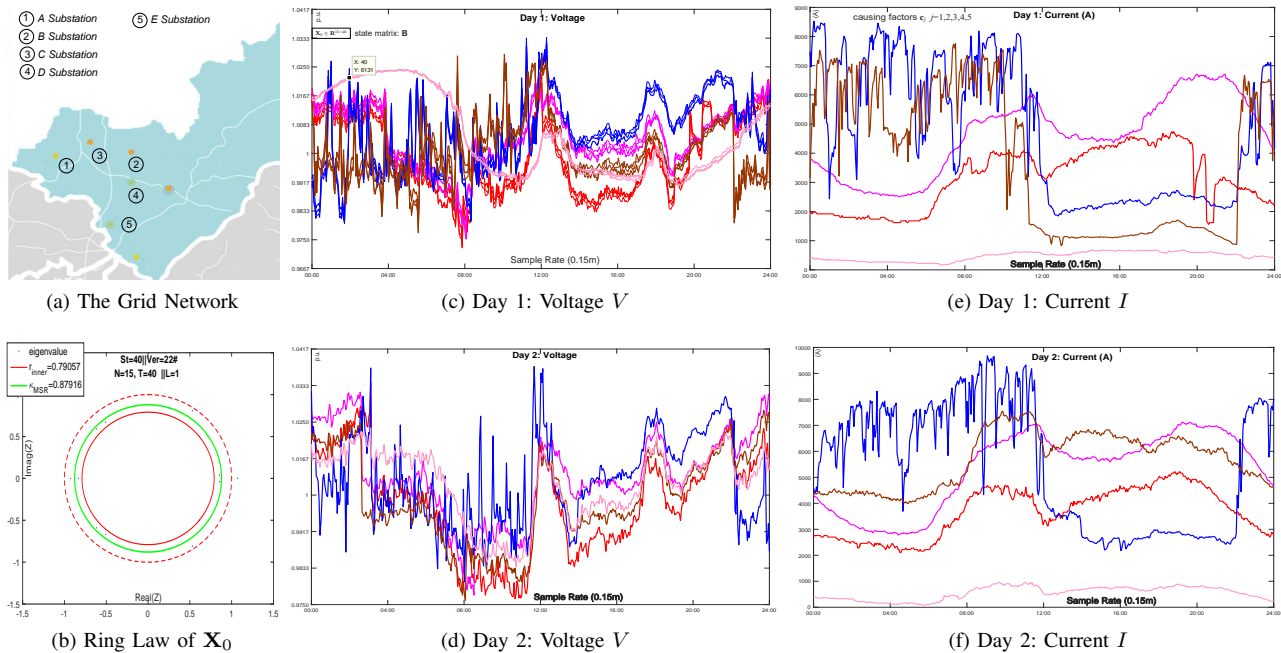


Fig. 6: Grid Network and Raw Data of Real Case

Note: For each substation, the 3-phase data are quite similar and only B-phase data are chosen.

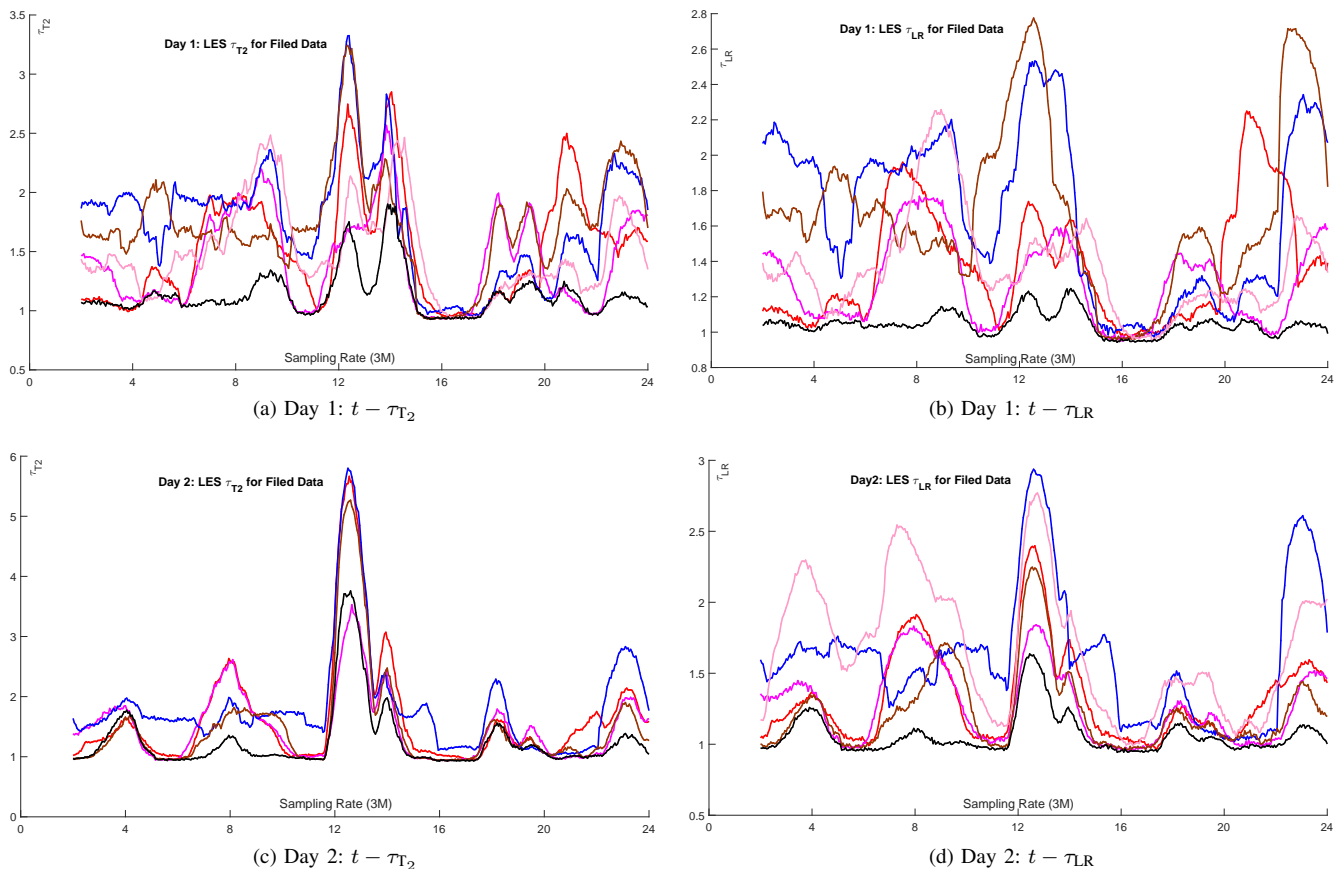


Fig. 7: Illusion of the LESs of field data.